doi:10.1093/brain/awy082 BRAIN 2018: 141; 1637–1649 | 1637

BRAIN
A JOURNAL OF NEUROLOGY

Spatiotemporal distribution of fibrinogen in marmoset and human inflammatory demyelination

Nathanael J. Lee,[1,2] Seung-Kwon Ha,[1] Pascal Sati,[1] Martina Absinta,[1] Nicholas J. Luciano,[1] Jennifer A. Lefeuvre,[1] Matthew K. Schindler,[1] Emily C. Leibovitch,[3] Jae Kyu Ryu,[4] Mark A. Petersen,[4,5] Afonso C. Silva,[6] Steven Jacobson,[3] Katerina Akassoglou[4,7] and Daniel S. Reich[1]

Multiple sclerosis is an inflammatory demyelinating disease of the central nervous system. Although it has been extensively studied, the proximate trigger of the immune response remains uncertain. Experimental autoimmune encephalomyelitis in the common marmoset recapitulates many radiological and pathological features of focal multiple sclerosis lesions in the cerebral white matter, unlike traditional experimental autoimmune encephalomyelitis in rodents. This provides an opportunity to investigate how lesions form as well as the relative timing of factors involved in lesion pathogenesis, especially during early stages of the disease. We used MRI to track experimental autoimmune encephalomyelitis lesions *in vivo* to determine their age, stage of development, and location, and we assessed the corresponding histopathology post-mortem. We focused on the plasma protein fibrinogen—a marker for blood–brain barrier leakage that has also been linked to a pathogenic role in inflammatory demyelinating lesion development. We show that fibrinogen has a specific spatiotemporal deposition pattern, apparently deriving from the central vein in early experimental autoimmune encephalomyelitis lesions <6 weeks old, and preceding both demyelination and visible gadolinium enhancement on MRI. Thus, fibrinogen leakage is one of the earliest detectable events in lesion pathogenesis. In slightly older lesions, fibrinogen is found inside microglia/macrophages, suggesting rapid phagocytosis. Quantification demonstrates positive correlation of fibrinogen deposition with accumulation of inflammatory cells, including microglia/macrophages and T cells. The peak of fibrinogen deposition coincides with the onset of demyelination and axonal loss. In samples from chronic multiple sclerosis cases, fibrinogen was found at the edge of chronic active lesions, which have ongoing demyelination and inflammation, but not in inactive lesions, suggesting that fibrinogen may play a role in sustained inflammation even in the chronic setting. In summary, our data support the notion that fibrinogen is a key player in the early pathogenesis, as well as sustained inflammation, of inflammatory demyelinating lesions.

1 Translational Neuroradiology Section, National Institute of Neurological Disorders and Stroke, National Institutes of Health, Bethesda, MD 20892, USA
2 Department of Neuroscience, Georgetown University Medical Center, Georgetown University, Washington, DC 20007, USA
3 Viral Immunology Section, National Institute of Neurological Disorders and Stroke, National Institutes of Health, Bethesda, MD 20892, USA
4 Gladstone Institutes, San Francisco, CA 94158, USA
5 Department of Pediatrics, University of California San Francisco, San Francisco, CA 94158, USA
6 Cerebral Microcirculation Section, National Institute of Neurological Disorders and Stroke, National Institutes of Health, Bethesda, MD 20892, USA
7 Department of Neurology, University of California San Francisco, San Francisco, CA 94158, USA

Received September 5, 2017. Revised January 8, 2018. Accepted February 4, 2018. Advance Access publication April 20, 2018

Correspondence to: Daniel S. Reich
Translational Neuroradiology Section, National Institute of Neurological Disorders and Stroke,
National Institutes of Health, Bethesda, MD 20892, USA
E-mail: daniel.reich@nih.gov

Keywords: common marmosets (*Callithrix jacchus*); multiple sclerosis; experimental autoimmune encephalomyelitis; fibrinogen; blood–brain barrier

Abbreviations: EAE = experimental autoimmune encephalomyelitis; NDIN = non-demyelinated inflammatory nodules

Introduction

Multiple sclerosis is an inflammatory demyelinating disease of the CNS in which myelin is damaged (Lassmann *et al.*, 2007). Multiple sclerosis patients develop characteristic lesions in the CNS that have different pathological features depending on the stage of lesion development. However, multiple sclerosis tissue is often not readily available for such pathological analyses. Experimental autoimmune encephalomyelitis (EAE) in the common marmoset (*Callithrix jacchus*) reproduces many pathological and radiological features of multiple sclerosis lesions in the white matter that are not evident in rodent models ('t Hart and Massacesi, 2009; Kap *et al.*, 2010; Maggi *et al.*, 2014, 2017; Absinta *et al.*, 2016); clinically, it recapitulates the relapsing-remitting clinical course of multiple sclerosis, which is the most prevalent type (Frohman *et al.*, 2006). Thus, the marmoset EAE model provides an opportunity to investigate how inflammatory demyelinating lesions develop, as well as the spatiotemporal dynamics of factors involved in lesion pathogenesis.

One of the hallmarks of multiple sclerosis, especially during the early stages of lesion pathophysiology, is alteration of the blood–brain barrier (Alvarez *et al.*, 2011, 2015; Schenk and de Vries, 2016), which allows immune cells from the periphery to enter the CNS, a key component of myelin and axon damage (Lassmann *et al.*, 2001; Dutta and Trapp, 2007). As one of the earliest events of multiple sclerosis lesion pathogenesis (Kermode *et al.*, 1990), blood–brain barrier opening, indicated by gadolinium enhancement on MRI (Runge *et al.*, 1985), can precede, or even occur independently from, a clinical relapse. Gadolinium has become a reliable marker for detecting early, often subclinical multiple sclerosis lesions (Harris *et al.*, 1991). However, some studies have also suggested that the blood–brain barrier is chronically damaged in chronic multiple sclerosis lesions, as indicated by immunohistochemistry of peripheral plasma proteins in the CNS (Kwon and Prineas, 1994; McQuaid *et al.*, 2009). Recent work on blood–brain barrier and gadolinium enhancement during lesion development further demonstrates that blood–brain barrier disruption is a dynamic process throughout lesion formation (Gaitán *et al.*, 2011). However, MRI does not identify the soluble factors—including cytokines and plasma proteins—that are involved in lesion development.

Fibrinogen, a plasma protein, can serve as a reliable immunohistochemical marker for blood–brain barrier leakage, but interestingly it has also been identified as having a pathogenic role in neurodegenerative diseases (Gay and Esiri, 1991; Claudio *et al.*, 1995; Vos *et al.*, 2005; Marik *et al.*, 2007; Cortes-Canteli *et al.*, 2012) and in multiple sclerosis lesion development (Ryu *et al.*, 2015; Petersen *et al.*, 2017; Yates *et al.*, 2017). In a rodent model, unlike other plasma proteins that may pass through a leaky blood–brain barrier such as albumin or kininogen, fibrinogen induces microglial activation, recruitment of peripheral macrophages, and inflammatory demyelination. Microglia release pro-inflammatory cytokines and chemokines that recruit peripheral cells of the adaptive immune system (particularly T cells) across the blood–brain barrier (Ryu *et al.*, 2015). Whether fibrinogen plays a role in lesion development in the marmoset EAE model, and the nature of any such role, has not been elucidated.

To investigate the role of fibrinogen in the pathogenesis of inflammatory demyelinating lesions, we first used serial *in vivo* proton density-weighted MRI to date the appearance of focal lesions in the white matter (Maggi *et al.*, 2014). Proton density-weighted images are highly sensitive to tissue damage and repair (Reich *et al.*, 2015). Guided by the *in vivo* MRI data and post-mortem MRI of the formalin-fixed brain, we performed histopathology to investigate factors (including fibrinogen, myelin markers, and inflammatory cells) that are present during each stage of lesion development, as well as their level of activity and distribution pattern. We also looked for fibrinogen deposition in both chronic active and chronic inactive multiple sclerosis lesions (Lassmann *et al.*, 1998; Kuhlmann *et al.*, 2017).

Materials and methods

Marmoset experimental autoimmune encephalomyelitis induction

We report exploratory analysis of data derived from eight marmosets (two males and six females, aged 2–5 years). All experimental animal protocols were approved by the Institutional Animal Care and Use Committee. Marmosets 1–7 received intradermal injections of 600 µl white matter homogenate emulsified in complete Freund's adjuvant, in four dorsal sites around the inguinal and axillary lymph nodes. The homogenate comprised 200 mg human white matter collected from an autopsy, which was homogenized and emulsified with 250 µl incomplete Freund's adjuvant (Difco Laboratories), minimal volumes of phosphate-buffered saline, and 1.8 mg desiccated heat-killed *Mycobacterium tuberculosis* (Difco Laboratories). Marmosets 1–7 were also involved in another study investigating the effects

of human herpes virus (HHV), thus some were co-immunized with HHV6A, HHV6B, or neither (Supplementary Table 1) via intranasal administration as described previously (Leibovitch *et al.*, 2013). Marmoset 8 was from a second protocol, and first received a half-dose of 100 mg human white matter homogenate. When no lesion appeared after 2 months, a full dose of 200 mg human white matter homogenate was introduced using the same method as marmosets 1–7. Marmoset 8 did not receive HHV6 immunization.

Marmoset *in vivo* MRI

Prior to scanning, marmosets were examined by neurologists to assess clinical symptoms, after which they were anesthetized, prepared, and scanned as described previously (Sati *et al.*, 2012). A proton density-weighted sequence was used to identify and track lesion development (Fig. 1A). T_1-weighted images were used for detecting gadolinium (gadobutrol, 0.3 mg/kg) leakage. Specific sequence parameters are listed in Supplementary Table 2.

Histopathology

Animals were necropsied within 1 h of death. Brains were collected and fixed in 4% paraformaldehyde. To precisely target brain regions of interest, we used customized 3D-printed brain cradles for each marmoset, as previously described (Guy *et al.*, 2016; Luciano *et al.*, 2016). Once the individual slabs were embedded in paraffin, they were cut into 4-µm thick slides and mounted on SuperFrost® Plus (Thermo Fisher Scientific) slides.

For human multiple sclerosis tissue, brains were collected at autopsy, fixed in formalin, embedded in paraffin, and cut into 7–10-µm thick slides. Relevant demographics are listed in Supplementary Table 3. Lesions were identified and targeted as previously described (Absinta *et al.*, 2014).

For histopathological stains on both marmoset and human tissue, slides were deparaffinized with xylene and rehydrated before staining. For Luxol fast blue staining to visualize myelin, slides were put in NovaUltra LFB Solution (IHC World) overnight at 56°C, differentiated with lithium carbonate, and counterstained with periodic acid-Schiff (IHC World). For Bielschowsky staining to visualize nerve fibres, slides were put in 10% silver nitrate solution, placed in ammonium silver solution at 40°C, and differentiated with concentrated ammonium hydroxide.

For immunohistochemistry, the immunoperoxidase staining method was used for ionized calcium binding adapter molecule-1 (Iba1; Wako Pure Chemical Industries; polyclonal), myeloid-related protein 14 (MRP14; Dako; monoclonal; clone MAC387), CD3 (Dako; polyclonal), aspartoacylase (ASPA; GeneTex; polyclonal), myelin proteolipid protein (PLP; Bio-Rad; monoclonal), CD68 (monocytes and macrophages; Dako; polyclonal), fibrinogen (kindly provided by Drs J. Degen and E. Mullins, Cincinnati, OH, USA; polyclonal), glial fibrillary acidic protein (GFAP; Dako; polyclonal), TMEM119 (MilliporeSigma; polyclonal), amyloid precursor protein (APP; MilliporeSigma; monoclonal; clone 22C11), non-phosphorylated neurofilament (SMI32; BioLegend; polyclonal), and phosphorylated neurofilament (SMI31; BioLegend; polyclonal). The alkaline phosphatase (AP) staining method was used for a second fibrinogen antibody (Abcam; monoclonal), MRP14 antibody used for double-staining, albumin (Abcam; monoclonal), dysferlin (Abcam; monoclonal), and oligodendrocyte transcription factor 2 (Olig2; Chemicon International; polyclonal). For immunoperoxidase staining, slides went through their respective antigen retrieval (Supplementary Table 4), were washed with hydrogen peroxide, and were incubated with the described protein blocking agents. Slides were then incubated with the relevant primary and secondary antibodies, and were developed using diaminobenzidine (Abcam). Slides were counterstained with Mayer's haematoxylin (IHC World), and differentiated with Blue Buffer (Leica Biosystems Inc.). For alkaline phosphatase staining, slides went through antigen retrieval, protein blocking, and primary and secondary antibody incubation (Supplementary Table 4), and were developed using AP Vector Blue (Vector Laboratories Inc.). Slides were then counterstained with Nuclear Fast Red solution (Abcam). For double-staining, e.g. with fibrinogen and Iba1, the immunoperoxidase staining method was applied first, followed by application of the alkaline phosphatase method without the antigen retrieval step or counterstain. All histopathological analysis and immunohistochemistry for fibrinogen and other markers on marmoset and human tissues were performed at NINDS. Fibrinogen immunohistochemistry on marmoset tissue was also independently confirmed at Gladstone Institutes.

Histopathological lesion characterization

After referencing histopathologically-identified lesions to prior *in vivo* MRI, the lesions were categorized into four groups: non-demyelinated inflammatory nodules (NDIN), which are seen only histopathologically and have no MRI counterpart (Maggi *et al.*, 2014); lesions 0–2 weeks; lesions between 2–6 weeks old; and lesions older than 6 weeks. Five healthy white matter areas, five NDINs, 11 0–2-week-old lesions, seven 2–6-week-old lesions, and 14 >6-week-old lesions, each collected from at least three individual marmosets, were analysed in this study.

Lesions from multiple sclerosis patients were classified into chronic active ($n = 4$) and chronic inactive ($n = 5$) according to international histological criteria (Lassmann *et al.*, 1998; Kuhlmann *et al.*, 2017).

Histological quantification and experimental design

All quantification was performed with Fiji ImageJ software. For PLP, Luxol fast blue, SMI31, Iba1, and MRP14 staining, the lesions went through colour deconvolution to remove counterstains, edge segmentation to avoid unwanted grey matter or ventricle, and thresholding to calculate the percentage area (Supplementary Fig. 1). In cases where individual cells could be counted, such as CD3, cell area was calculated by manually counting the cells within each lesion. For method validation, quantification of CD3+ cell area and percentage area were compared, yielding no significant difference. For normal white matter, lesion-free regions contralateral to areas with common lesion appearance (such as the optic radiation) were chosen. For fibrinogen deposition, scoring criteria were established (Table 1 and Supplementary Fig. 2). The descriptions of fibrinogen deposition patterns were determined based on our own experience in marmoset EAE, as well as that of other investigators who have described fibrinogen deposition in the context of blood–brain barrier leakage (Davalos *et al.*, 2012; Nacer *et al.*, 2012; Shikani *et al.*, 2012). Each section was examined and interpreted

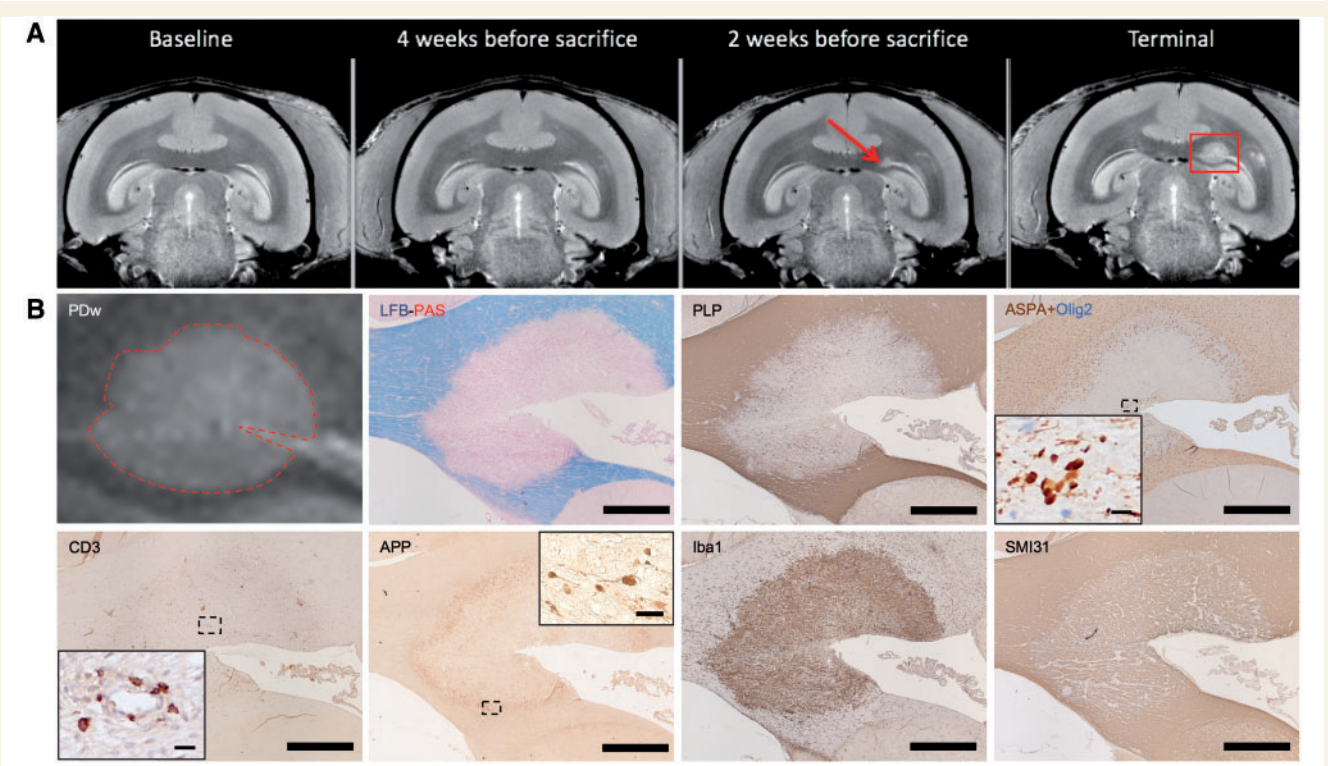

Figure 1 Characterization of marmoset EAE lesions using MRI and histopathology. (**A**) Serial *in vivo* proton density-weighted (PDw) MRI dates evolution of a periventricular white matter lesion. Red arrow = first lesion appearance on MRI; red box = lesion at terminal MRI. (**B**) Multimodal histological and immunohistochemical analysis of the same lesion, shown in magnified view on interpolated MRI (dotted red line). Luxol fast blue-periodic acid-Schiff (LFB-PAS) and PLP = myelin; ASPA + Olig2 = oligodendrocytes (brown: mature oligodendrocytes; blue: progenitors); CD3 = T cells; APP = degenerating axons; Iba1 = microglia/macrophages; SMI31 = phosphorylated neurofilament (mostly found in intact axons). IHC counterstain with haematoxylin. Scale bar = 100 μm; insets = 10 μm. Lesion selected from marmoset 4.

by a board-certified veterinary pathologist who was blinded to lesion category and marmoset identification. Intra- and inter-rater reliability were tested with a secondary reviewer, which confirmed high reliability (Cohen's Kappa $\geqslant 0.941$). Images were taken using a Zeiss Observer 1 microscope (Zeiss) and ZEN blue software (Zeiss).

Statistical analysis

For comparison across multiple lesion categories, the non-parametric Kruskal-Wallis test was used. Simple linear regression and goodness of fit were used to analyse correlations. $P < 0.05$ was considered statistically significant. For intra- and inter-rater reliability, Cohen's Kappa test was performed. All statistical analyses were performed with GraphPad Prism 7 software.

Results

Fibrinogen is found in early, active experimental autoimmune encephalomyelitis lesions

As fibrinogen has been investigated to be necessary and sufficient for early pathogenesis of inflammatory demyelination in rodents (Davalos *et al.*, 2012; Ryu *et al.*, 2015) but not in non-human primates, we investigated the spatiotemporal dynamics of fibrinogen deposition in marmoset EAE by creating a radiology-to-pathology linkage (Fig. 1A and B). Our data from 37 lesions in eight marmosets demonstrate that fibrinogen is mainly detected in the early stages of lesion development, specifically in the NDINs that precede demyelination, 0–2-week-old lesions, 2–6-week-old lesions, and minimally in >6-week-old lesions (Fig. 2A). This finding was confirmed using two different fibrinogen antibodies (Fig. 2B). When all 37 lesions were analysed based on the fibrinogen deposition criteria (Table 1 and Supplementary Fig. 2), 0–2-week-old lesions were found to have the greatest amount of fibrinogen deposition, followed by 2–6-week-old lesions and NDIN (Fig. 2C). Other plasma proteins that have been investigated as markers of blood–brain barrier leakage in the context of multiple sclerosis, specifically albumin and dysferlin (Hochmeister *et al.*, 2006; Schoderboeck *et al.*, 2009; LeVine 2016), demonstrated no specific spatiotemporal pattern in EAE lesions (Supplementary Fig. 3).

Fibrinogen first leaks into the parenchyma and is then quickly phagocytized by microglia and macrophages

Since fibrinogen has been reported to interact with microglia in CNS (Marik *et al.*, 2007; Ryu *et al.*, 2015), we

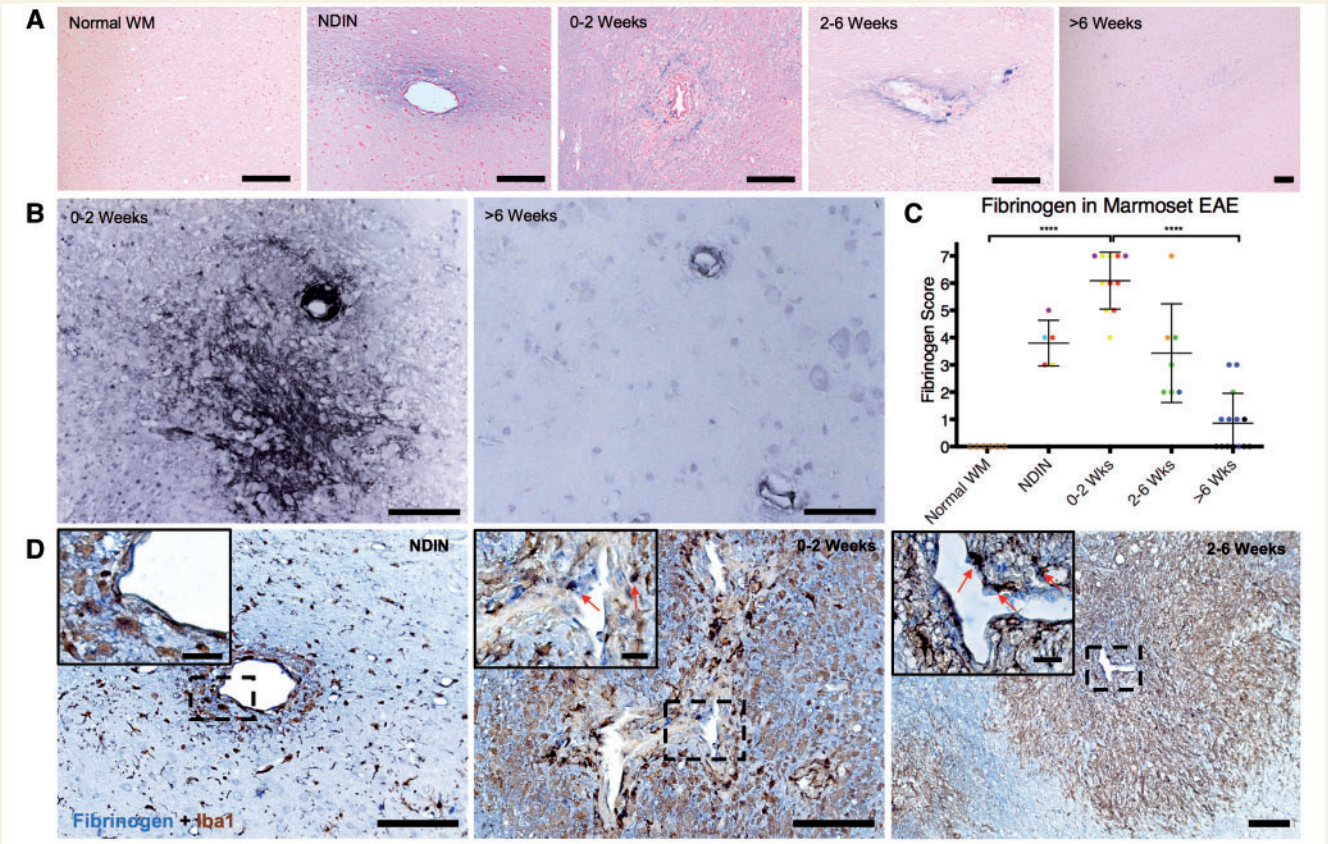

Figure 2 Fibrinogen deposition throughout marmoset EAE lesion development. (**A**) Fibrinogen (blue) is detected in non-demyelinating inflammatory nodules (NDIN), 0–2 and 2–6-week-old lesions around the veins in the center of the lesions, but not in >6-week-old lesions or normal white matter. Counterstain = nuclear fast red. (**B**) Fibrinogen (black) deposition pattern is validated using polyclonal fibrinogen antibody, where fibrinogen deposition is extensive in 0–2-week-old EAE lesions, but not in >6-week-old lesions. Counterstain = haematoxylin. (**C**) Quantification of fibrinogen deposition based on fibrinogen deposition scoring criteria (see also Table 1 and Supplementary Fig. 2). Points represent individual lesions, and are colour-coded based on Supplementary Table 1. (**D**) Fibrinogen/Iba1 double-staining shows that fibrinogen (blue) is deposited in proximity to Iba1 + microglia/macrophages (brown) in the parenchyma. EAE lesions 0–2 and 2–6 weeks old harbour intracellular fibrinogen (red arrows) within Iba1 + cells. Scale bar = 100 μm; scale bar inside boxes = 20 μm. ****$P < 0.0001$ (Kruskal-Wallis test). Lesions selected from marmosets 1, 3, 4, and 6.

Table 1 Scoring criteria for fibrinogen deposition

	Score	Criteria description
Extracellular deposition	0	No sign of fibrinogen leakage
	1	Minimal deposition, just detectable along the vessel wall
	2	Slight deposition around the vessel wall
	3	Moderate deposition in the parenchyma
	4	Marked deposition in the parenchyma surrounding vessel
	5	Severe, extensive deposition in the parenchyma
Intracellular deposition	0	No intracellular fibrinogen
	1	Scattered intracellular deposition (one to several foci)
	2	Extensive intracellular deposition
Total	0–7	

investigated the localization of fibrinogen at different stages of lesion development, specifically in relation to Iba1 + microglia/macrophage distribution. Fibrinogen and Iba1 double-staining shows that fibrinogen first leaks into the parenchyma during the NDIN stage of lesion development, in which fibrinogen and microglia/macrophages are both present, but with only rare examples of fibrinogen localization within microglia/macrophages (Fig. 2D). However, in 0–2 and 2–6-week-old lesions, fibrinogen is much more commonly found inside microglia/macrophages (Fig. 2D), suggesting that these cells quickly react to fibrinogen extravasation, resulting in rapid phagocytosis.

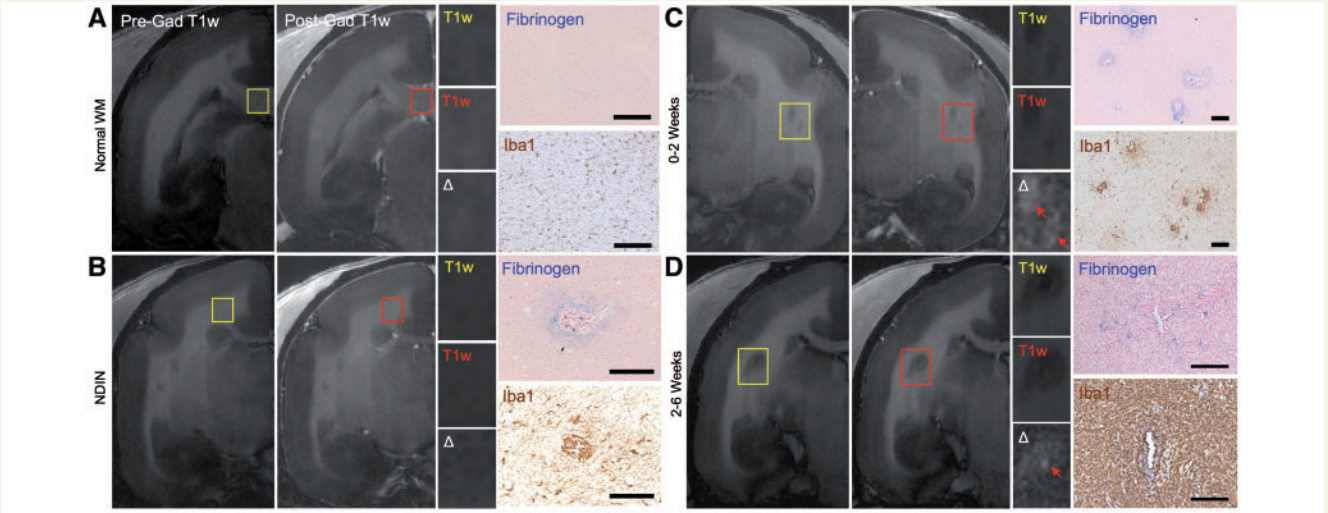

Figure 3 Terminal *in vivo* MRI and immunohistochemistry of blood-brain barrier leakage in marmoset EAE lesions. (**A**) Pre- (yellow) and post- (red) gadolinium (Gad) T_1-weighted (T1w) images, and fibrinogen (blue) and Iba1 (brown) staining of normal white matter. (**B**) An NDIN, invisible on both the terminal pre- and post-gadolinium T_1-weighted images, has active blood–brain barrier leakage based on fibrinogen staining, and inflammation based on Iba1 staining. (**C**) 0–2-week-old and (**D**) 2–6-week-old EAE lesions are visible on T_1-weighted images and show active gadolinium leakage through a leaky blood–brain barrier, as indicated by subtle gadolinium leakage (red arrows) on subtraction images (Δ = post − pre gad). Immunohistochemistry confirms that both fibrinogen deposition and inflammation (Iba1) are found in lesions with active gadolinium leakage. Fibrinogen counterstain = nuclear fast red; Iba1 counterstain = haematoxylin. Scale bar = 100 μm. Lesions selected from marmosets 2 and 7.

Fibrinogen deposits before demyelination and gadolinium leakage, and peaks when demyelination starts

Fibrinogen deposition was not detected in normal white matter (Fig. 3A) but was seen in NDIN, which are invisible on MRI and show no gadolinium leakage (Fig. 3B). As expected, the earliest lesions showed subtle gadolinium leakage (both 0–2 and 2–6-week-old lesions) (Fig. 3C and D). We also investigated the spatiotemporal relation between fibrinogen and other markers of disease activity, including markers of demyelination, oligodendrocytes, and astrocytes. Our data show that the peak of fibrinogen deposition, which occurs during the first two weeks of lesion development, coincides with the onset of active demyelination (Fig. 4A–C). These lesions also harbour activated astrocytes (Fig. 4A). Both the mature oligodendrocytes and oligodendrocyte precursor cell populations significantly decrease, but at later time windows (2–6 weeks and >6 weeks after lesion formation, respectively) (Fig. 4A, D and E).

Fibrinogen deposition correlates with inflammatory cell accumulation

In addition to Iba1+ microglia/macrophages, we investigated the spatiotemporal relation between fibrinogen and other markers of inflammatory cells, including MRP14+ early activated peripheral macrophages and CD3+ T cells. Our data show that fibrinogen leakage during the initial stages of lesion development, specifically during the NDIN stages and the first 6 weeks of EAE, coincides with a significant increase in inflammatory cells, including Iba1+ microglia/macrophages, MRP14+ early activated peripheral macrophages, and CD3+ T cells (Fig. 5A–D). We further investigated the spatiotemporal relation of TMEM119, a recently discovered specific marker of microglia (Bennett *et al.*, 2016; Satoh *et al.*, 2016), in relation to Iba1+ and MRP14+ cells, and show that TMEM119+ microglia are not present during the first 2 weeks of lesion development, and do not spatially overlap with MRP14+ cells (Fig. 5A). However, Iba1+ cells were present wherever TMEM119+ microglia were found. Furthermore, Iba1 staining shows that many Iba1+ microglia/macrophages fail to express either TMEM119 or MPR14. These data suggest that brain-derived TMEM119+ microglia and peripherally derived MRP14+ are indeed separate groups of inflammatory cells in EAE lesion development, but also that there are many other innate immune cells that require further characterization. Throughout the entirety of lesion development, fibrinogen deposition is positively correlated with inflammatory cell density (Fig. 5E–G).

The peak of fibrinogen deposition coincides with the onset of axonal damage and loss

As axonal damage and loss are among the hallmarks of multiple sclerosis lesions, we investigated the relation between fibrinogen deposition and various markers of axonal injury. Our data show that the peak of fibrinogen deposition, which is during the first 2 weeks of lesion formation, coincides with axonal damage and loss. During the 0–2-week window, there

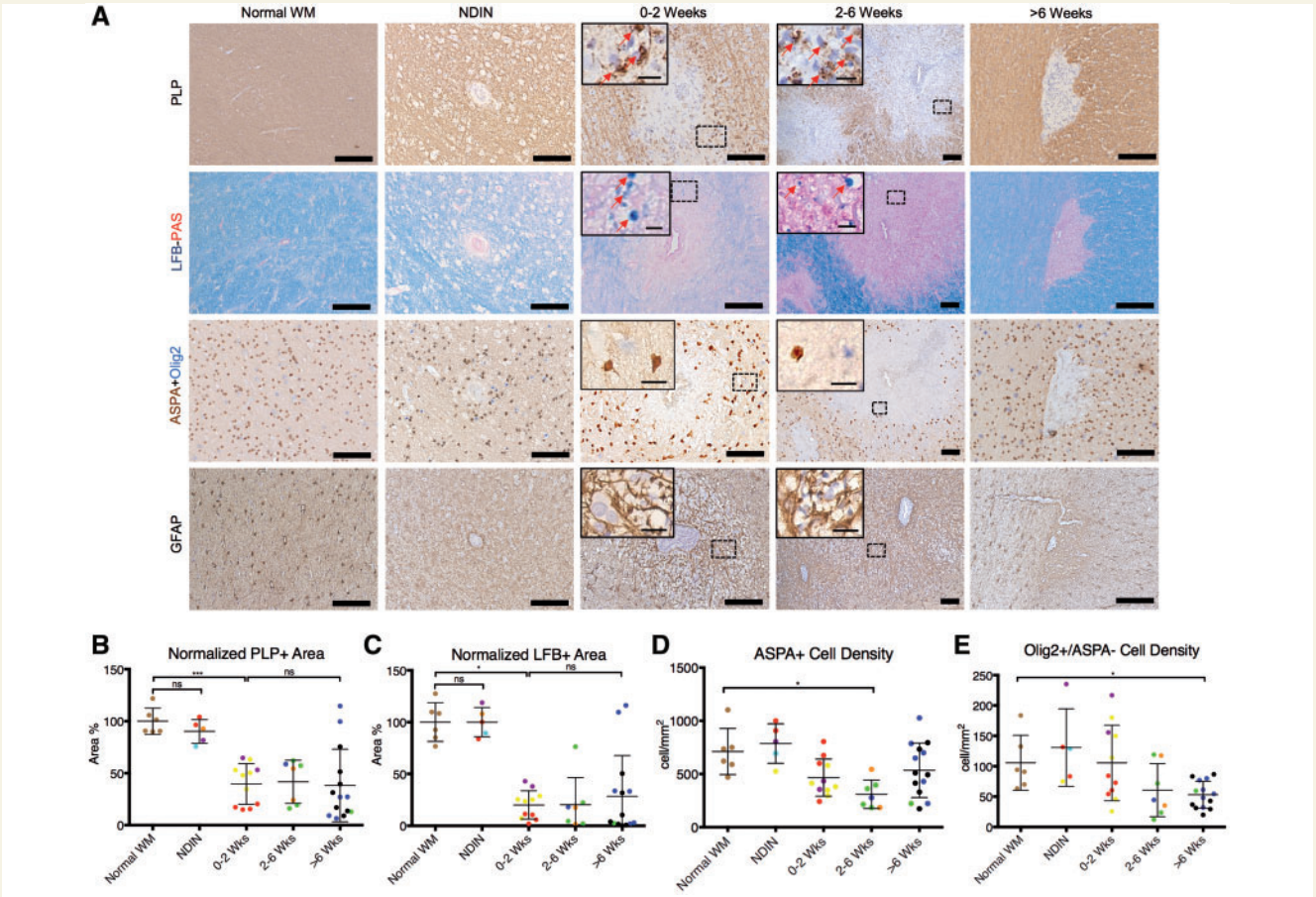

Figure 4 Immunostaining for myelin, oligodendrocytes, and astrocytes in marmoset EAE lesions, categorized based on age. (**A**) Staining for PLP and Luxol fast blue (LFB) shows that active demyelination takes place during the first 2 weeks of EAE lesion development, represented by intracellular myelin debris inside phagocytes (red arrows). Double-staining for ASPA + Olig2 shows that ASPA + mature oligodendrocytes and Olig2 + /ASPA− oligodendrocyte progenitors decrease after the peak of active demyelination. Immunostaining for GFAP shows that astrocytes are activated from early in lesion development, mostly from the first 2 weeks, and stay activated until the chronic phase. Quantification of (**B**) PLP and (**C**) Luxol fast blue, based on normalized area percentage, shows that lesions are demyelinated from the time they appear on MRI, and most remain demyelinated. Quantification of (**D**) ASPA + and (**E**) Olig2 + /ASPA- cells demonstrates that mature oligodendrocytes are significantly reduced in number by 2-6 weeks after lesion formation, whereas oligodendrocyte progenitors decline more slowly. Dots represent individual lesions and are colour-coded based on Supplementary Table 1. PLP and GFAP counterstain = haematoxylin; Luxol fast blue counterstain = periodic acid-Schiff. Scale bar = 100 μm; scale bar inside boxes = 10 μm. ns = not significant; *$P < 0.05$; ***$P < 0.001$ (Kruskal-Wallis test). Lesions selected from marmosets 2, 3, 5, and 7.

was a significant increase in the number of APP + elements in the lesions, which represent acute axonal injury (Fig. 6A and B); appearance of SMI32 + ovoid bodies, which represent non-phosphorylated neurofilaments that are not found in normal white matter (Fig. 6A); loss of SMI31 + phosphorylated neurofilaments (Fig. 6A and C); and loss of nerve fibres by Bielschowsky silver stain. Axonal injury and loss persisted throughout the entirety of lesion development (Fig. 6A–C).

Chronic active multiple sclerosis lesions harbour fibrinogen, but chronic inactive lesions do not

To verify the involvement of fibrinogen in the pathophysiology of inflammatory demyelination in humans further, we investigated nine multiple sclerosis lesions in four brains. Our results demonstrate that fibrinogen extravasation was seen in three of the four chronic active white matter lesions, but none of the five chronic inactive white matter lesions analysed (Fig. 7A and B). In chronic active lesions, fibrinogen localized specifically around the blood vessels at the lesion edge, where active demyelination and sustained inflammation were also present (Fig. 7A). In fibrinogen-positive chronic active lesions, most (range: 67–86%) of the blood vessels at the lesion edge showed evidence of fibrinogen deposition (Supplementary Table 5). In none of the multiple sclerosis lesions were blood vessels at the lesion centre permeable to fibrinogen.

Discussion

The earliest events of inflammatory demyelinating lesion pathogenesis, especially the initial triggers of microglial

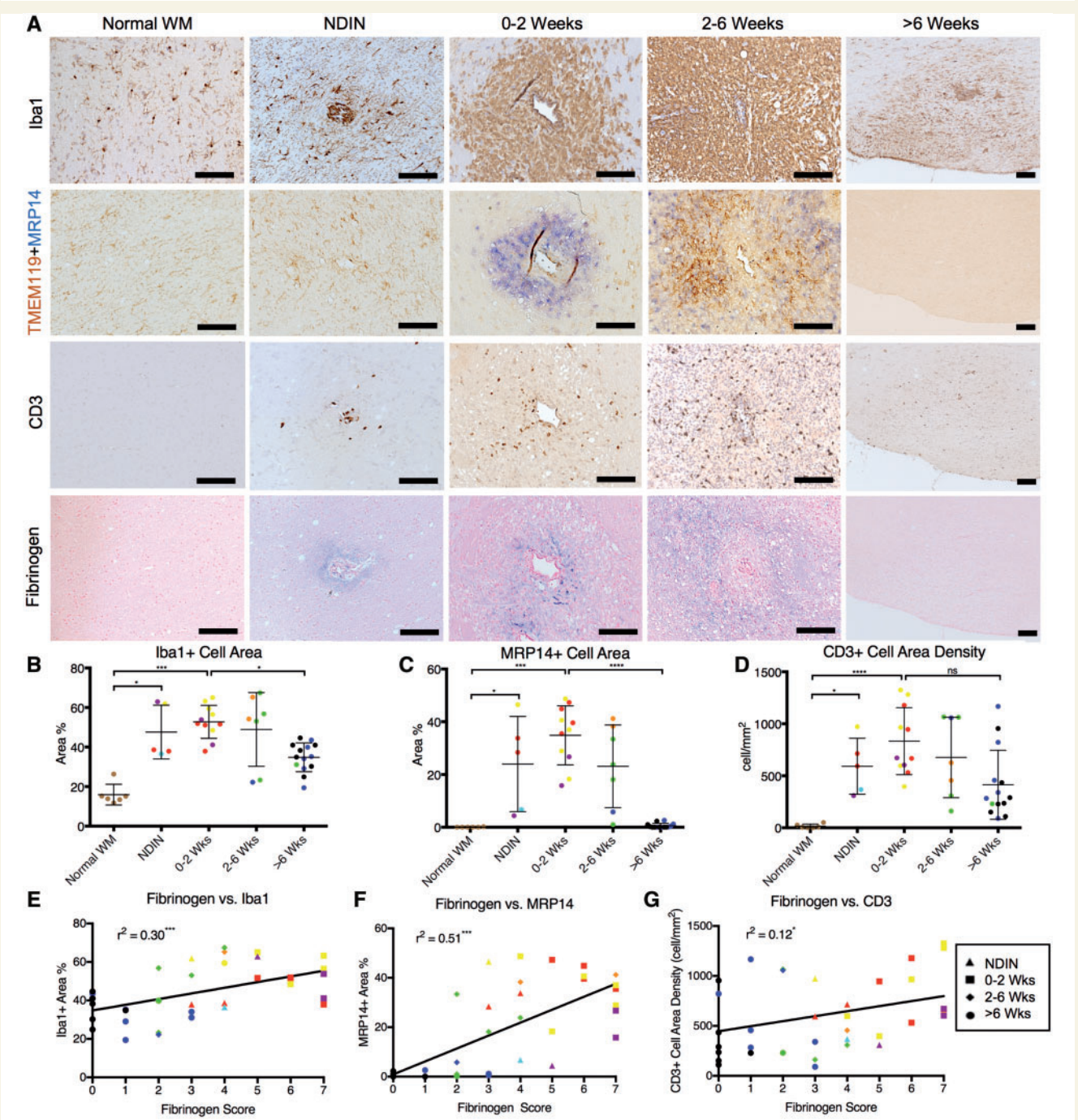

Figure 5 Inflammation and fibrinogen in marmoset EAE lesions, categorized based on age. (**A**) Immunohistochemistry of Iba1 (microglia/macrophages), TMEM119 (microglia) + MRP14 (early activated peripheral macrophages), CD3 (T cells), and fibrinogen in EAE lesions. TMEM119 + MRP14 double-staining demonstrates that MRP14 + macrophages are distinct from TMEM119 + microglia. Iba1 + staining demonstrates that there are Iba1 + cells that stain for neither TMEM119 nor MRP14. (**B**) Iba1 +, (**C**) MRP14 +, and (**D**) CD3 + cells are present from early lesion development during the non-demyelinating inflammatory nodule (NDIN) stage, preceding demyelination. All three types of inflammatory cells peak during the first 2 weeks of EAE lesion development, and decrease as lesions age. Fibrinogen deposition is positively correlated, albeit imperfectly, with the amount of (**E**) Iba1 +, (**F**) MRP14 +, and (**G**) CD3 + cells throughout lesion development, suggesting that inflammation and fibrinogen deposition have similar time courses. Individual lesions are represented by points, which are colour-coded based on Supplementary Table 1. Counterstain = haematoxylin. Scale bar = 100 μm. ns = not significant; *$P < 0.05$; **$P < 0.005$; ***$P < 0.001$; ****$P < 0.0001$ (Kruskal-Wallis test). Lesions selected from marmosets 1, 2, 6, and 7.

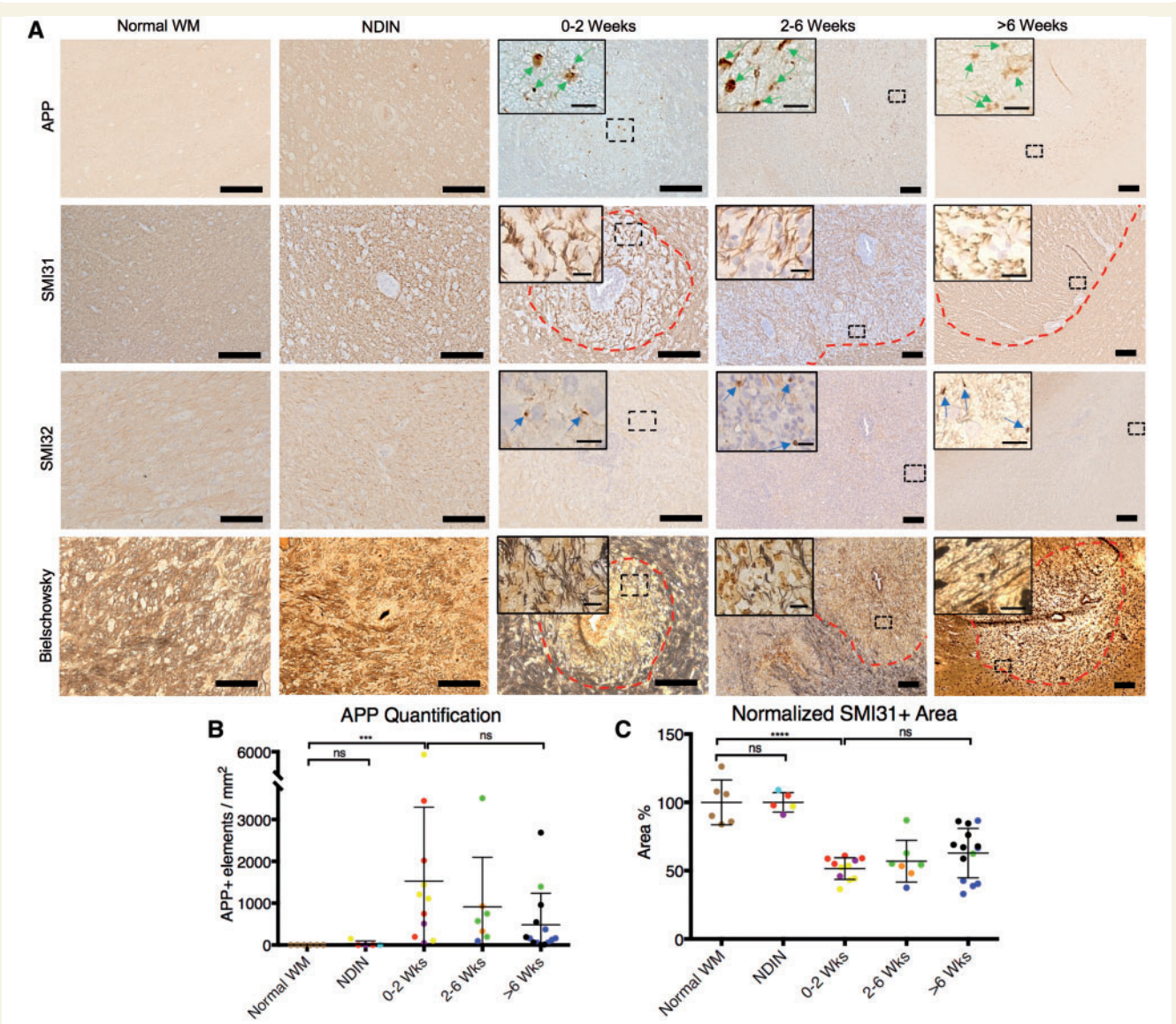

Figure 6 Healthy and damaged axons in marmoset EAE lesions, categorized based on lesion age. (**A**) Staining for APP (acute axonal damage), SMI31 (phosphorylated neurofilament), SMI32 (non-phosphorylated neurofilament), and Bielschowsky silver stain (nerve fibres) shows that axonal damage and axonal loss takes place during the first two weeks of EAE lesion development, which coincides with the peak of fibrinogen deposition, represented by the presence of APP+ elements (green arrows) and SMI32+ ovoid bodies (blue arrows), as well as loss of axon fibres and phosphorylated neurofilaments. (**B**) Counts of APP+ elements and (**C**) quantification of SMI31 staining, based on normalized area percentage, show that acute axonal damage and loss can be seen throughout lesion development. Dots represent individual lesions, and are color-coded based on Supplementary Table 1. Dotted red lines = lesion edge. SMI31 and SMI32 counterstain = hematoxylin. Scale bar = 100 μm; scale bar inside boxes = 10 μm. ns = not significant; ***$P < 0.001$; ****$P < 0.0001$ (Kruskal-Wallis test). Lesions selected from marmosets 2, 3, 4, and 5.

and astrocytic activation and recruitment of peripheral leucocytes, are only beginning to be understood. Recent studies in rodents have shown that fibrinogen leaks out of blood vessels and, once converted to fibrin, can bind microglia via the CD11b receptor, causing release of pro-inflammatory cytokines that prime the immune system to recruit peripheral immune cells to enter the CNS and cause demyelination (Adams *et al.*, 2007; Davalos *et al.*, 2012; Ryu *et al.*, 2015). Introducing fibrinogen, but not other plasma proteins such as albumin, into healthy white matter of susceptible mice was sufficient to cause inflammatory demyelination, and blocking the binding of fibrinogen to microglia prevented fibrinogen-induced demyelination (Ryu *et al.*, 2015). Our findings in the marmoset model—in particular the timing of fibrinogen appearance in relation to demyelination, its interaction with microglia/macrophages, and its correlation with inflammatory cell accumulation—support the notion that fibrinogen plays a key role.

Our data show that fibrinogen is found in early, active lesions during the first 6 weeks of lesion development. The fibrinogen deposition score correlates with accumulation of

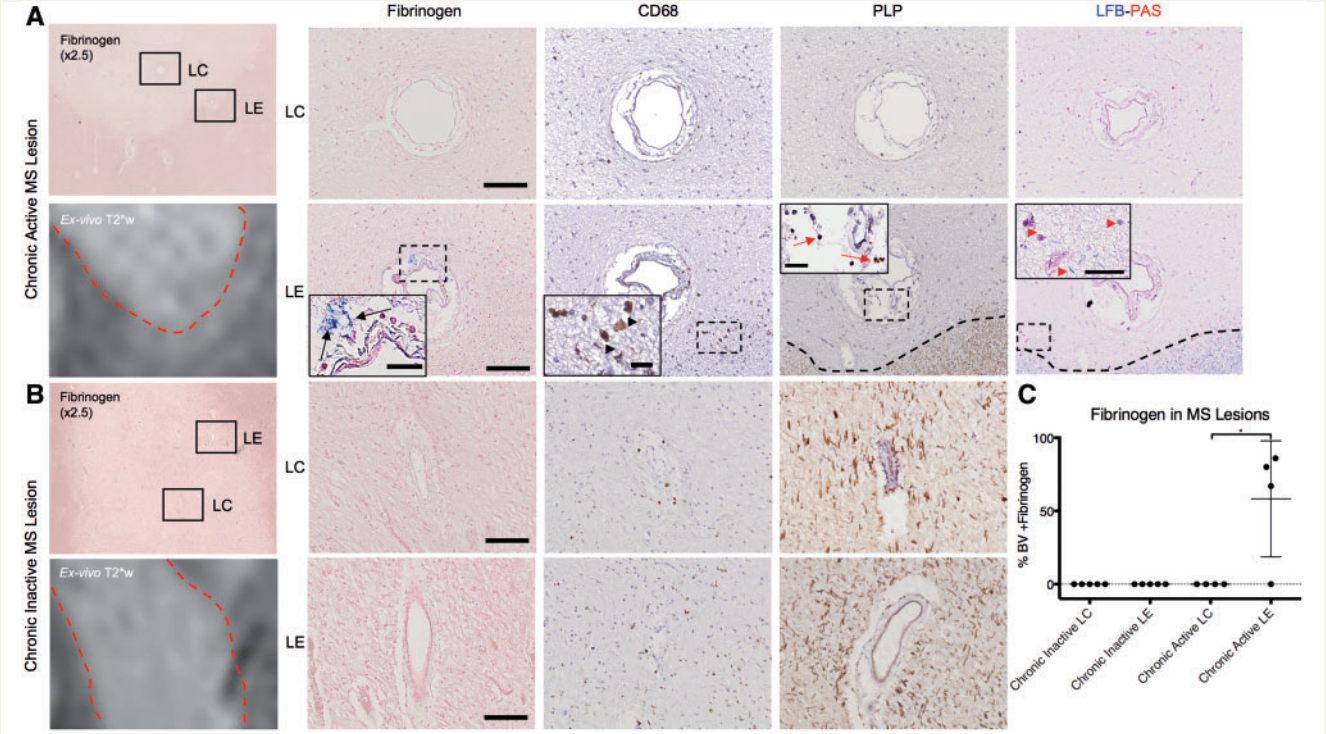

Figure 7 Fibrinogen deposition in human multiple sclerosis lesions. Histology is juxtaposed to *ex vivo* T2*-weighted MRI scans of the same lesions. (**A**) Fibrinogen (blue) is found around blood vessels (BV; black arrows) located at chronic active lesion edge (LE), but not the lesion centre (LC). Areas around these vessels show inflammation and ongoing demyelination, indicated by the presence of CD68 + cells (black arrowheads), and intracellular myelin proteolipid protein (red arrows) and periodic acid-Schiff + myelin breakdown products (red arrowheads). (**B**) Fibrinogen is not detected in either the edge or the centre of chronic inactive lesions. (**C**) Percentage of blood vessels with fibrinogen deposition. Three of four chronic active lesions, from two individuals, had fibrinogen deposition within the majority of blood vessels at the lesion edge, but none in the centre. None of the five chronic inactive lesions assayed, from two individuals, showed fibrinogen deposition. Fibrinogen counterstain = nuclear fast red; PLP and CD68 counterstain = haematoxylin. Scale bar = 100 μm; insets = 20 μm. *$P < 0.05$ (Kruskal-Wallis test).

inflammatory cells, including microglia, macrophages, and T cells. Fibrinogen is observed to leak out of a lesion's central vein at the earliest stage of lesion development, which we term the NDIN stage, and which precedes demyelination and gadolinium enhancement. Fibrinogen is then quickly phagocytized by microglia/macrophages as the lesions develop. When fibrinogen deposition is at its peak during the first two weeks of lesion development, lesions are actively demyelinated and show axonal injury and loss, and astrocytic activation. On the other hand, since we observed T cells and fibrinogen in all NDINs analysed, unlike in our prior study (Maggi *et al.*, 2014), we cannot rule out the possibility that T cell infiltration precedes (and perhaps initiates) blood–brain barrier opening. Indeed, the absence of demyelination in NDINs does not exclude T cell infiltration as the inciting event; in a rodent model, the entry of CNS-irrelevant T cells into the brain can cause blood–brain barrier disruption (Smorodchenko *et al.*, 2007), which opens the door to fibrinogen deposition and the cascade of innate and adaptive myelin-specific immune responses mentioned above. Differentiating CNS-irrelevant and -specific T cells *in situ* would therefore be important for elucidating the precise sequence of events in inflammatory demyelinating lesion pathogenesis.

We also investigated the involvement of other plasma proteins (dysferlin and albumin) and show that they do not share the same spatiotemporal distribution pattern as fibrinogen. This may be because fibrinogen specifically binds to microglia/macrophages in the brain as demonstrated previously, whereas other plasma proteins do not (Ryu *et al.*, 2015). Differences in distribution between fibrinogen and other plasma proteins might also be due to different mechanisms of clearance of fibrinogen and fibrin from the CNS (Bardehle *et al.*, 2015). In contrast to other blood proteins, fibrinogen is converted to insoluble fibrin in the CNS and its main mechanism for removal is proteolytic degradation via tissue plasminogen activator (tPA)/plasmin (Bardehle *et al.*, 2015). Phagocytosis has been described as a clearance mechanism of fibrin in tissues (Motley *et al.*, 2016). Impaired clearance of fibrin has been reported in multiple sclerosis (Gveric *et al.*, 2003) and might contribute to sustained fibrin deposition and thus differences in spatiotemporal distribution with respect to other blood proteins that do not form insoluble deposits in the CNS. Investigating additional serum proteins, such as

immunoglobulins, as well as other molecules involved in the neurovascular unit that governs the brain's permeability to such plasma proteins and may affect the inflammatory demyelinating processes (Kirk *et al.*, 2003; Bennett *et al.*, 2010), would be an important next step for validating the specificity of fibrinogen's involvement in early lesion formation.

To confirm a role for fibrinogen in inflammatory demyelination further, we also investigated the distribution of fibrinogen in human multiple sclerosis tissue. We focused on chronic lesions, as time-resolved acute lesions similar to those studied in the marmoset model were not available. Our data from four chronic active and five chronic inactive multiple sclerosis lesions suggest that fibrinogen is specifically deposited at the edge of chronic active multiple sclerosis lesions, where histopathologic evidence of smoldering demyelination and inflammation are present, but not in chronic inactive lesions. The majority of vessels at the edge of most chronic active lesions showed fibrinogen deposition, whereas none of the vessels in the centres of those lesions, or in chronic inactive lesions—in both of which astrogliosis is the primary pathological observation—harboured fibrinogen. Other studies have previously detected fibrin in chronic inactive lesions by electron microscopy (Claudio *et al.*, 1995) and immunohistochemistry (Vos *et al.*, 2005; Leech *et al.*, 2007). It is possible that lesion heterogeneity or differences in tissue fixation and antibody preparation might influence the sensitivity of detection in tissues with low fibrin levels. These results suggest that chronic active lesions may have subtle blood–brain barrier disruption that is associated with active demyelination, as suggested by prior histopathological (Kwon and Prineas, 1994; McQuaid *et al.*, 2009) and MRI-based studies (Hawkins *et al.*, 1990; Katz *et al.*, 1993; Silver *et al.*, 2001). Alternatively, fibrinogen deposition at the site of disease activity may indicate failure to remove previously deposited fibrinogen or fibrin, which may in turn be a cause of ongoing demyelination, sustained inflammation, and inhibition of remyelination. Regardless of the pathophysiology, our findings suggest that targeting fibrinogen in sustained inflammatory demyelinating lesions may be therapeutic. In fact, by blocking microglia from binding fibrinogen through targeting CD11b receptors, or by depleting fibrinogen through the defibrinogenating agent ancrod, demyelination was reduced (Adams *et al.*, 2007; Ryu *et al.*, 2015). Furthermore, our findings showing fibrinogen deposition prior to gadolinium enhancement by MRI suggest that sensitive probes for early detection of fibrinogen and fibrin might be useful imaging tools for early detection of multiple sclerosis lesions (Davalos *et al.*, 2014; Bain *et al.*, 2018).

The disruption of the blood–brain barrier in multiple sclerosis and EAE, and the association between fibrinogen extravasation into the parenchyma and inflammatory demyelination, beg the question of whether this event is specific to multiple sclerosis. There are other diseases of the CNS with blood–brain barrier abnormalities and fibrin deposition, such as stroke and Alzheimer's Disease (Tomimoto *et al.*, 1996; Sandoval and Witt, 2008; Erickson and Banks, 2013; Cortes-Canteli *et al.*, 2015; Kassner and Merali, 2015), that do not harbour the same phenotype and pathophysiology of multiple sclerosis lesions. One possible explanation might be that fibrinogen has to be present within a host with genetic susceptibility to autoimmune disease. Autoimmune inflammatory demyelination requires specific immunologic environments and key players. Indeed, in rodent models, it has been reported that fibrinogen selectively recruits myelin-specific T cells from the periphery into the CNS, but fails to recruit T cells in ovalbumin-specific T cell receptor transgenic mice, demonstrating that myelin-specific T cells need to be readily available in order for fibrinogen to initiate the demyelination cascade (Ryu *et al.*, 2015). Last but not least, it is well known that multiple sclerosis is a highly heterogeneous disease with various disease courses, pathways, and lesion pathologies (Lucchinetti *et al.*, 2004; Lassmann, 2005; Disanto *et al.*, 2011; Dendrou *et al.*, 2015; Reich *et al.*, 2018). Blood–brain barrier disruption is a common denominator of disease pathogenesis in multiple sclerosis. It is possible that fibrin may play a crucial role in stages of the disease with active blood–brain barrier leakage. Fibrin is the final product of the coagulation cascade and also undergoes active fibrinolysis at sites of lesions. Indeed, the fibrinolytic potential in multiple sclerosis lesions is markedly decreased and proteins that inhibit fibrinolysis, such as PAI-1, correlate with neuronal loss in progressive multiple sclerosis (Gveric *et al.*, 2003; Yates *et al.*, 2017). In EAE, fibrin is required for both early inflammation and development of axonal damage at later disease stages (Davalos *et al.*, 2012). Patient heterogeneity in the balance between coagulable states and fibrinolytic pathways may determine the contribution of fibrin to disease pathogenesis in chronic disease states.

One of the limitations to the current study is that the persistent activation of microglia/macrophages and smoldering demyelination, which are typical of human chronic active lesions, are not properly recapitulated by the acute marmoset EAE model used here. Unfortunately, there is no ideal model for chronic active lesions, but such a model would be of great value for understanding the role of fibrinogen and the therapeutic implications of blocking it. An additional limitation is that we cannot rule out the possibility that herpesvirus inoculation may have affected the course of the lesion formation in our model. Our previous study demonstrated that intranasal administration of either HHV6A or HHV6B in marmosets only resulted in negligible virus-specific antibody responses that were clinically asymptomatic (Leibovitch *et al.*, 2013).

Overall, our data are consistent with the notion that fibrinogen is involved in the early pathogenesis of inflammatory demyelinating lesions and is also tightly linked to sustained inflammation in longstanding disease. This study provides several novel insights into the overall pathophysiology of inflammatory demyelination and further supports

that possibility that fibrinogen may be an effective therapeutic target for countering the initiation and sustainment of inflammatory demyelination.

Acknowledgement

We thank Dr Govind Nair for *ex vivo* MRI of the human tissue.

Funding

This research was partially supported by the Intramural Research Program of NINDS; NIH/NICHD K12-HD000850 to M.A.P.; A Race to Erase MS Young Investigator Award and American Heart Association Scientist Development Grant 16SDG30170014 to J.K.R.; Georgetown University Medical Center Graduate Student Organization Student Research Grants Program to N.J.L.; NMSS fellowship award #FG 2093-A-1 and Marilyn Hilton Bridging Award for Physician-Scientists from the Conrad N. Hilton Foundation grant #EIN 15-20858115 to M.A.; NMSS Clinician Scientist award #FAN 17103-A-1 to M.K.S.; and a Conrad N. Hilton Foundation grant 17348, NMSS research grant RG4985A3/1, and NIH/NINDS R35 NS097976 to K.A.

Conflicts of interest

The authors declare competing financial interests. K.A. is a co-founder of MedaRed, Inc and K.A. and J.K.R. are named inventors on patents and patent applications related to fibrin. Their interests are managed by the Gladstone Institutes in accordance with its conflict of interest policy.

Supplementary material

Supplementary material is available at *Brain* online.

References

Absinta M, Nair G, Filippi M, Ray-Chaudhury A, Reyes-Mantilla MI, Pardo CA, et al. Postmortem magnetic resonance imaging to guide the pathologic cut: individualized, 3-dimensionally printed cutting boxes for fixed brains. J Neuropathol Exp Neurol 2014; 73: 780–8.

Absinta M, Sati P, Reich DS. Advanced MRI and staging of multiple sclerosis lesions. Nat Rev Neurol 2016; 12: 358–68.

Adams RA, Bauer J, Flick MJ, Sikorski SL, Nuriel T, Lassmann H, et al. The fibrin-derived gamma377-395 peptide inhibits microglia activation and suppresses relapsing paralysis in central nervous system autoimmune disease. J Exp Med 2007; 204: 571–82.

Alvarez JI, Cayrol R, Prat A. Disruption of central nervous system barriers in multiple sclerosis. Biochim Biophys Acta 2011; 1812: 252–64.

Alvarez JI, Saint-Laurent O, Godschalk A, Terouz S, Briels C, Larouche S, et al. Focal disturbances in the blood-brain barrier are associated with formation of neuroinflammatory lesions. Neurobiol Dis 2015; 74: 14–24.

Bain LJ, Keren NI, Norris SM. Biomarkers of neuroinflammation. Washington, DC: National Academies Press; 2018. p. 1–90.

Bardehle S, Rafalski VA, Akassoglou K. Breaking boundaries-coagulation and fibrinolysis at the neurovascular interface. Front Cell Neurosci 2015; 9: 354.

Bennett J, Basivireddy J, Kollar A, Biron KE, Reickmann P, Jefferies WA, et al. Blood-brain barrier disruption and enhanced vascular permeability in the multiple sclerosis model EAE. J Neuroimmunol 2010; 229: 180–91.

Bennett ML, Bennett FC, Liddelow SA, Ajami B, Zamanian JL, Fernhoff NB, et al. New tools for studying microglia in the mouse and human CNS. Proc Natl Acad Sci USA 2016; 113: E1738–46.

Claudio L, Raine CS, Brosnan CF. Evidence of persistent blood-brain barrier abnormalities in chronic-progressive multiple sclerosis. Acta Neuropathol 1995; 90: 228–38.

Cortes-Canteli M, Mattei L, Richards AT, Norris EH, Strickland S. Fibrin deposited in the Alzheimer's disease brain promotes neuronal degeneration. Neurobiol Aging 2015; 36: 608–17.

Cortes-Canteli M, Zamolodchikov D, Ahn HJ, Strickland S, Norris EH. Fibrinogen and altered hemostasis in Alzheimer's disease. J Alzheimers Dis 2012; 32: 599–608.

Davalos D, Baeten KM, Whitney MA, Mullins ES, Friedman B, Olson ES, et al. Early detection of thrombin activity in neuroinflammatory disease. Ann Neurol 2014; 75: 303–8.

Davalos D, Ryu JK, Merlini M, Baeten KM, Le Moan N, Petersen MA, et al. Fibrinogen-induced perivascular microglial clustering is required for the development of axonal damage in neuroinflammation. Nat Commun 2012; 3: 1227.

Dendrou CA, Fugger L, Friese MA. Immunopathology of multiple sclerosis. Nat Rev Immunol 2015; 15: 545–58.

Disanto G, Berlanga AJ, Handel AE, Para AE, Burrell AM, Fries A, et al. Heterogeneity in multiple sclerosis: scratching the surface of a complex disease. Autoimmune Dis 2011; 2011: 932351.

Dutta R, Trapp BD. Pathogenesis of axonal and neuronal damage in multiple sclerosis. Neurology 2007; 68 (22 Suppl 3): S22–31; discussion S43–54.

Erickson MA, Banks WA. Blood-brain barrier dysfunction as a cause and consequence of Alzheimer's disease. J Cereb Blood Flow Metab 2013; 33: 1500–13.

Frohman EM, Racke MK, Raine CS. Multiple sclerosis–the plaque and its pathogenesis. N Engl J Med 2006; 354: 942–55.

Gaitán MI, Shea CD, Evangelou IE, Stone RD, Fenton KM, Bielekova B, et al. Evolution of the blood-brain barrier in newly forming multiple sclerosis lesions. Ann Neurol 2011; 70: 22–9.

Gay D, Esiri M. Blood-brain barrier damage in acute multiple sclerosis plaques. An immunocytological study. Brain 1991; 114 (Pt 1B): 557–72.

Guy JR, Sati P, Leibovitch E, Jacobson S, Silva AC, Reich DS. Custom fit 3D-printed brain holders for comparison of histology with MRI in marmosets. J Neurosci Methods 2016; 257: 55–63.

Gveric D, Herrera B, Petzold A, Lawrence DA, Cuzner ML. Impaired fibrinolysis in multiple sclerosis: a role for tissue plasminogen activator inhibitors. Brain 2003; 126 (Pt 7): 1590–8.

Harris JO, Frank JA, Patronas N, McFarlin DE, McFarland HF. Serial gadolinium-enhanced magnetic resonance imaging scans in patients with early, relapsing-remitting multiple sclerosis: implications for clinical trials and natural history. Ann Neurol 1991; 29: 548–55.

Hawkins CP, Munro PM, MacKenzie F, Kesselring J, Tofts PS, du Boulay EP, et al. Duration and selectivity of blood-brain barrier breakdown in chronic relapsing experimental allergic encephalomyelitis studied by gadolinium-DTPA and protein markers. Brain 1990; 113 (Pt 2): 365–78.

Hochmeister S, Grundtner R, Bauer J, Engelhardt B, Lyck R, Gordon G, et al. Dysferlin is a new marker for leaky brain blood vessels in multiple sclerosis. J Neuropathol Exp Neurol 2006; 65: 855–65.

Kap YS, Laman JD, 't Hart BA. Experimental autoimmune encephalomyelitis in the common marmoset, a bridge between rodent EAE and multiple sclerosis for immunotherapy development. J Neuroimmune Pharmacol 2010; 5: 220–30.

Kassner A, Merali Z. Assessment of blood-brain barrier disruption in stroke. Stroke 2015; 46: 3310–15.

Katz D, Taubenberger JK, Cannella B, McFarlin DE, Raine CS, McFarland HF. Correlation between magnetic resonance imaging findings and lesion development in chronic, active multiple sclerosis. Ann Neurol 1993; 34: 661–9.

Kermode AG, Thompson AJ, Tofts P, MacManus DG, Kendall BE, Kingsley DP, et al. Breakdown of the blood-brain barrier precedes symptoms and other MRI signs of new lesions in multiple sclerosis. Pathogenetic and clinical implications. Brain 1990; 113 (Pt 5): 1477–89.

Kirk J, Plumb J, Mirakhur M, McQuaid S. Tight junctional abnormality in multiple sclerosis white matter affects all calibres of vessel and is associated with blood-brain barrier leakage and active demyelination. J Pathol 2003; 201: 319–27.

Kuhlmann T, Ludwin S, Prat A, Antel J, Brück W, Lassmann H. An updated histological classification system for multiple sclerosis lesions. Acta Neuropathol 2017; 133: 13–24.

Kwon EE, Prineas JW. Blood-brain barrier abnormalities in longstanding multiple sclerosis lesions. An immunohistochemical study. J Neuropathol Exp Neurol 1994; 53: 625–36.

Lassmann H. Heterogeneity of multiple sclerosis: implications for therapy targeting regeneration. Ernst Schering Res Found Workshop 2005; 53: 11–22.

Lassmann H, Brück W, Lucchinetti C. Heterogeneity of multiple sclerosis pathogenesis: implications for diagnosis and therapy. Trends Mol Med 2001; 7: 115–21.

Lassmann H, Brück W, Lucchinetti CF. The immunopathology of multiple sclerosis: an overview. Brain Pathol 2007; 17: 210–18.

Lassmann H, Raine CS, Antel J, Prineas JW. Immunopathology of multiple sclerosis: report on an international meeting held at the Institute of Neurology of the University of Vienna. J Neuroimmunol 1998; 86: 213–17.

Leech S, Kirk J, Plumb J, McQuaid S. Persistent endothelial abnormalities and blood-brain barrier leak in primary and secondary progressive multiple sclerosis. Neuropathol Appl Neurobiol 2007; 33: 86–98.

Leibovitch E, Wohler JE, Cummings Macri SM, Motanic K, Harberts E, Gaitán MI, et al. Novel marmoset (Callithrix jacchus) model of human Herpesvirus 6A and 6B infections: immunologic, virologic and radiologic characterization. PLoS Pathog 2013; 9: e1003138.

LeVine SM. Albumin and multiple sclerosis. BMC Neurol 2016; 16: 47.

Lucchinetti CF, Brück W, Lassmann H. Evidence for pathogenic heterogeneity in multiple sclerosis. Ann Neurol 2004; 56: 308.

Luciano NJ, Sati P, Nair G, Guy JR, Ha SK, Absinta M, et al. Utilizing 3D printing technology to merge MRI with histology: a protocol for brain sectioning. J Vis Exp 2016; 118: 54780.

Maggi P, Macri SM, Gaitán MI, Leibovitch E, Wholer JE, Knight HL, et al. The formation of inflammatory demyelinated lesions in cerebral white matter. Ann Neurol 2014; 76: 594–608.

Maggi P, Sati P, Massacesi L. Magnetic resonance imaging of experimental autoimmune encephalomyelitis in the common marmoset. J Neuroimmunol 2017; 304: 86–92.

Marik C, Felts PA, Bauer J, Lassmann H, Smith KJ. Lesion genesis in a subset of patients with multiple sclerosis: a role for innate immunity? Brain 2007; 130 (Pt 11): 2800–15.

McQuaid S, Cunnea P, McMahon J, Fitzgerald U. The effects of blood-brain barrier disruption on glial cell function in multiple sclerosis. Biochem Soc Trans 2009; 37 (Pt 1): 329–31.

Motley MP, Madsen DH, Jürgensen HJ, Spencer DE, Szabo R, Holmbeck K, et al. A CCR2 macrophage endocytic pathway mediates extravascular fibrin clearance *in vivo*. Blood 2016; 127: 1085–96.

Nacer A, Movila A, Baer K, Mikolajczak SA, Kappe SH, Frevert U. Neuroimmunological blood brain barrier opening in experimental cerebral malaria. PLoS Pathog 2012; 8: e1002982.

Petersen MA, Ryu JK, Chang KJ, Etxeberria A, Bardehle S, Mendiola AS, et al. Fibrinogen activates BMP signaling in oligodendrocyte progenitor cells and inhibits remyelination after vascular damage. Neuron 2017; 96: 1003–12.e7.

Reich DS, Lucchinetti CF, Calabresi PA. Multiple sclerosis. N Engl J Med 2018; 378: 169–80.

Reich DS, White R, Cortese IC, Vuolo L, Shea CD, Collins TL, et al. Sample-size calculations for short-term proof-of-concept studies of tissue protection and repair in multiple sclerosis lesions via conventional clinical imaging. Mult Scler 2015; 21: 1693–704.

Runge VM, Schoerner W, Niendorf HP, Laniado M, Koehler D, Claussen C, et al. Initial clinical evaluation of gadolinium DTPA for contrast-enhanced magnetic resonance imaging. Magn Reson Imaging 1985; 3: 27–35.

Ryu JK, Petersen MA, Murray SG, Baeten KM, Meyer-Franke A, Chan JP, et al. Blood coagulation protein fibrinogen promotes autoimmunity and demyelination via chemokine release and antigen presentation. Nat Commun 2015; 6: 8164.

Sandoval KE, Witt KA. Blood-brain barrier tight junction permeability and ischemic stroke. Neurobiol Dis 2008; 32: 200–19.

Sati P, Silva AC, van Gelderen P, Gaitan MI, Wohler JE, Jacobson S, et al. *In vivo* quantification of T_2 anisotropy in white matter fibers in marmoset monkeys. Neuroimage 2012; 59: 979–85.

Satoh J, Kino Y, Asahina N, Takitani M, Miyoshi J, Ishida T, et al. TMEM119 marks a subset of microglia in the human brain. Neuropathology 2016; 36: 39–49.

Schenk GJ, de Vries HE. Altered blood-brain barrier transport in neuro-inflammatory disorders. Drug Discov Today Technol 2016; 20: 5–11.

Schoderboeck L, Adzemovic M, Nicolussi EM, Crupinschi C, Hochmeister S, Fischer MT, et al. The window of susceptibility for inflammation in the immature central nervous system is characterized by a leaky blood-brain barrier and the local expression of inflammatory chemokines. Neurobiol Dis 2009; 35: 368–75.

Shikani HJ, Freeman BD, Lisanti MP, Weiss LM, Tanowitz HB, Desruisseaux MS. Cerebral malaria: we have come a long way. Am J Pathol 2012; 181: 1484–92.

Silver NC, Tofts PS, Symms MR, Barker GJ, Thompson AJ, Miller DH. Quantitative contrast-enhanced magnetic resonance imaging to evaluate blood-brain barrier integrity in multiple sclerosis: a preliminary study. Mult Scler 2001; 7: 75–82.

Smorodchenko A, Wuerfel J, Pohl EE, Vogt J, Tysiak E, Glumm R, et al. CNS-irrelevant T-cells enter the brain, cause blood-brain barrier disruption but no glial pathology. Eur J Neurosci 2007; 26: 1387–98.

't Hart BA, Massacesi L. Clinical, pathological, and immunologic aspects of the multiple sclerosis model in common marmosets (Callithrix jacchus). J Neuropathol Exp Neurol 2009; 68: 341–55.

Tomimoto H, Akiguchi I, Suenaga T, Nishimura M, Wakita H, Nakamura S, et al. Alterations of the blood-brain barrier and glial cells in white-matter lesions in cerebrovascular and Alzheimer's disease patients. Stroke 1996; 27: 2069–74.

Vos CM, Geurts JJ, Montagne L, van Haastert ES, Bö L, van der Valk P, et al. Blood-brain barrier alterations in both focal and diffuse abnormalities on postmortem MRI in multiple sclerosis. Neurobiol Dis 2005; 20: 953–60.

Yates RL, Esiri MM, Palace J, Jacobs B, Perera R, DeLuca GC. Fibrin(ogen) and neurodegeneration in the progressive multiple sclerosis cortex. Ann Neurol 2017; 82: 259–70.